

## Exciton spectroscopy of hexagonal boron nitride using nonresonant x-ray Raman scattering

Yejun Feng,<sup>1,\*</sup> J. A. Soininen,<sup>2</sup> A. L. Ankudinov,<sup>3</sup> J. O. Cross,<sup>1</sup> G. T. Seidler,<sup>3,†</sup> A. T. Macrander,<sup>1</sup> J. J. Rehr,<sup>3</sup> and E. L. Shirley<sup>4</sup><sup>1</sup>Advanced Photon Source, Argonne National Laboratory, Argonne, Illinois 60439, USA<sup>2</sup>Department of Physical Science, University of Helsinki, Helsinki FIN-00014, Finland<sup>3</sup>Department of Physics, University of Washington, Seattle, Washington 98195, USA<sup>4</sup>Optical Technology Division, NIST, Gaithersburg, Maryland 20899, USA

(Received 3 October 2007; revised manuscript received 5 February 2008; published 8 April 2008)

We report nonresonant x-ray Raman scattering (XRS) measurements on the boron  $K$  edge of hexagonal boron nitride for transferred momentum ( $\mathbf{q}$ ) from 2 to 9  $\text{\AA}^{-1}$  along directions both in and out of the basal plane. A symmetry-based argument, together with real-space full multiple scattering calculations of the projected density of states in the spherical harmonics basis, reveals that a strong pre-edge feature is a dominantly  $Y_{10}$ -type exciton with no other  $s$ ,  $p$ , or  $d$  components. This conclusion is supported by a second, independent calculation of the  $\mathbf{q}$ -dependent XRS cross section based on the Bethe-Salpeter equation. This study demonstrates methods which should be applicable to the determination of final-state symmetries for localized resonances in other  $\mathbf{q}$ -dependent XRS studies of anisotropic single-crystal systems.

DOI: 10.1103/PhysRevB.77.165202

PACS number(s): 71.35.-y, 61.05.cj

## I. INTRODUCTION

The physics of low-energy photoelectrons in solids is a complex, many body problem.<sup>1</sup> All aspects of the electronic structure of the material must be taken into account,<sup>2,3</sup> including the interaction between the photoelectron and the complementary hole.<sup>3-6</sup> This latter effect allows for similar long-lived bound states in metals (generally called Fermi-edge singularities)<sup>7</sup> and in insulators (called excitons).<sup>8</sup> As a canonical example of a many body problem in condensed matter physics, core excitons are a topic of continuing interest.<sup>4-6</sup>

The present synergy between steadily progressing *ab initio* theoretical treatments<sup>2,3,9,10</sup> and on-going improvements in instrumentation<sup>11</sup> in studies of nonresonant x-ray Raman scattering (XRS) shows a strong potential for rapid progress on this old problem.<sup>5,6</sup> XRS is the inelastic scattering of hard x rays from bound electrons, and XRS studies have seen a recent explosion in the number and range of applications.<sup>5,6,11-18</sup> In comparison with  $\mathbf{q}$ -resolved electron energy loss spectroscopy (EELS),<sup>19</sup> XRS is more suited for bulk condensed matter systems<sup>13</sup> due to the large penetration length afforded by the relative high-energy incident and scattered photons. The measured  $\mathbf{q}$ -dependent XRS provides direct information about multipole contributions to the dynamic structure factor  $S(\mathbf{q}, \omega)$ .<sup>5,6,14-16</sup> It can be directly compared with theoretical calculations of  $S(\mathbf{q}, \omega)$ ,<sup>6,14-16</sup> and can in some cases be inverted to provide an experimental measure of the perturbed projected density of states ( $l$ -DOS),<sup>10,20</sup> which can again be compared to theory.

XRS has shown itself to be especially suitable for spectroscopy of the angular characteristics of core excitons at the near edge region. For example, XRS studies<sup>5,6</sup> on LiF and icosahedral  $B_4C$  convincingly demonstrated  $s$ - and  $p$ -type excitons at the F and B  $K$  edges, respectively, which can be attributed to atoms located at a center of inversion symmetry of the unit cell with parity a good quantum number for the final states.<sup>6</sup> Here, we demonstrate that for some systems one

can learn not only the  $\Delta l$  selection rule for the exciton but also a full description of its angular characteristics in terms of spherical harmonics  $Y_{lm}$ .

We present measurements of the  $\mathbf{q}$  dependent XRS on the boron  $K$  edge of hexagonal boron nitride ( $h$ -BN), an anisotropic system with all atoms sitting at positions with reflection symmetry to the basal plane (Fig. 1, inset).<sup>21</sup> The anisotropy of the dipole-limit core excitation spectra for  $\mathbf{q} \parallel c$  and  $\mathbf{q} \perp c$  for  $h$ -BN is well known from previous EELS,<sup>22</sup> XANES,<sup>23,24</sup> and XRS<sup>25</sup> studies at the  $q=0$  limit. We extend on this prior work by measuring the  $\mathbf{q}$ -dependent boron XRS for both  $\mathbf{q} \parallel c$  and  $\mathbf{q} \perp c$  out to  $q=9 \text{ \AA}^{-1}$ , a momentum transfer that is clearly beyond the dipole limit for the B  $1s$  initial state. By expanding the final state wave function onto the spherical harmonics basis, we identify a predominantly  $Y_{10}$ -type exciton in the pre-edge region. This qualitative, symmetry-based approach should be generally applicable when considering localized resonances in  $\mathbf{q}$ -dependent XRS studies of anisotropic single crystal systems. Two independent *ab initio* calculations, one of the perturbed  $l$ -DOS and the other a direct calculation of the  $\mathbf{q}$ -dependent XRS, confirm this identification of the angular dependence of the exciton's final state wave function.

## II. EXPERIMENTAL METHOD AND RESULTS

Our sample is highly oriented compression-annealed pyrolytic  $h$ -BN (Advanced Ceramics Research)<sup>26</sup> with dimensions  $14 \times 5 \times 0.9 \text{ mm}^3$ . The crystallite size is of the order of 1000  $\text{\AA}$  with a mosaic spread about  $2^\circ$  to  $3^\circ$  along the  $c$  axis.<sup>25</sup> The orientation within the basal plane is assumed to be random. All measurements were performed at the XOR/PNC-20-ID beamline of the Advanced Photon Source at Argonne National Laboratory. An 11.4-cm-diameter spherically bent Si (5, 5, 5) crystal analyzer was mounted in the vertical scattering plane on the arm of a Huber diffractometer, forming a near-backscattering Bragg diffraction geometry with the Amptek Si-PIN photodiode detector just above the

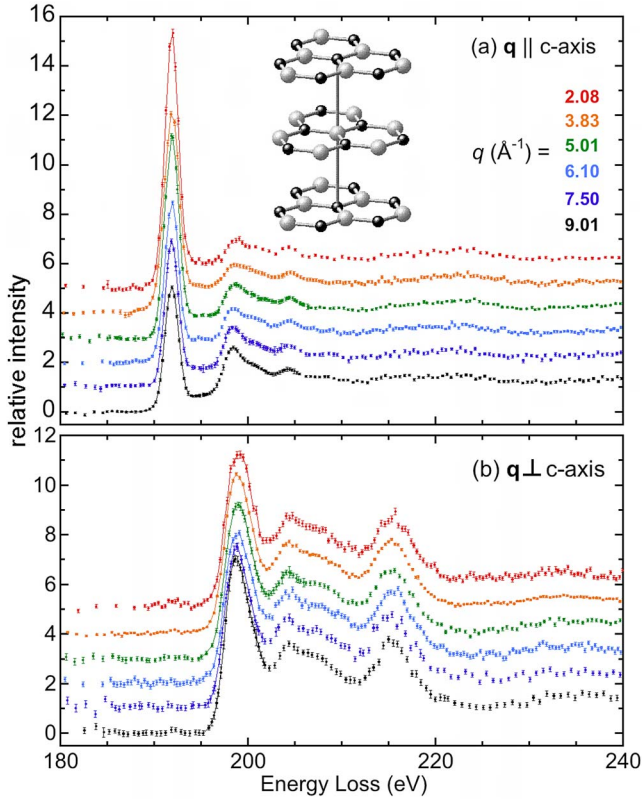


FIG. 1. (Color online) Inset: The crystalline structure of *h*-BN has two-dimensional hexagonal sheets stacked directly on top of each other, with the boron (black) and nitrogen (gray) always being nearest neighbors (Ref. 21). Main figure: The normalized XRS spectra from *h*-BN for  $\mathbf{q} \parallel c$  (top panel) and  $\mathbf{q} \perp c$  (bottom panel).

sample position. The incident x-ray energy was scanned with the x-ray analyzer energy fixed at 9890 eV. Henceforth, we refer to all energies in terms of energy loss with respect to the elastic scattering peak. Inelastic x-ray scattering spectra were measured at  $q=2.08, 3.83, 5.01, 6.10, 7.50,$  and  $9.01 \text{ \AA}^{-1}$  for directions parallel and perpendicular to the *c* axis, with a resolution varying from 0.25 to  $0.11 \text{ \AA}^{-1}$ . Further details of our apparatus have been reported elsewhere.<sup>6,27</sup> All of the elastic peaks are fit well by a Gaussian function, defining the energy resolution to be between 1.32 and 1.66 eV FWHM with the broadening a consequence of the different effective sample size as a function of scattering angle. The data were numerically broadened, as necessary, to the maximum resolution of 1.66 eV FWHM for visual comparison.

The observed energy-loss spectra include inelastic scattering from both the core and the valence electrons, corresponding to the *K* edge XRS and the Compton scattering, respectively. The separation of the XRS signal from the larger Compton background is a key experimental difficulty in all XRS measurements.<sup>16,28</sup> The valence Compton backgrounds are approximated by fitting the pre-edge data to standard Compton forms and using the low-*q* limit XRS form as a reference.<sup>27</sup>

The resulting boron XRS spectra are presented in Fig. 1. The pre-edge peak position is  $191.9 \pm 0.1 \text{ eV}$  for the *c* axis spectra, and the main edge peak position is  $198.8 \pm 0.1 \text{ eV}$

along both directions, consistent with prior work using other experimental methods.<sup>22–25</sup> All of the spectra were normalized according to the integrated intensity in the 210 to 250 eV range, mimicking the *f*-sum rule, and naturally introducing a  $q^2$  factor.<sup>29</sup> The resulting XRS spectra are shown in Fig. 1 for both  $\mathbf{q} \parallel c$  (top panel) and  $\mathbf{q} \perp c$  (bottom panel).

### III. DISCUSSION

Previous experimental studies have suggested that the physical origin of the pre-edge peak in *h*-BN is a core exciton.<sup>23,30</sup> Theoretical calculations have confirmed this notion by demonstrating the importance of the interaction between the core-hole and the photoelectron.<sup>31</sup> In the XRS spectra for  $\mathbf{q} \parallel c$  (Fig. 1, top panel) this exciton state exhibits a prominent monotonically decreasing peak intensity with increasing *q*. Another less obvious but equally significant feature is the total absence of the exciton peak in spectra measured within the basal plane for any *q* values. Although the shape and intensity of the main edge peaks along both directions also display subtle variations, we concentrate on the behavior of the exciton.

We now present a general formalism for  $\mathbf{q}$ -dependent XRS in order to understand the interplay between the final-state characteristics measured by core-exciton spectroscopy and the local symmetry at the sites of interest. The dynamic structure factor  $S(\mathbf{q}, \omega)$  is expressed in a single-electron picture as

$$S(\mathbf{q}, \omega) = \sum_f |\langle f | e^{i\mathbf{q}\cdot\mathbf{r}} | 0 \rangle|^2 \delta(\Delta E - \hbar\omega). \quad (1)$$

Following the short-range order theory<sup>33</sup> due to the localized core-hole effect and the general guideline of Doniach *et al.*,<sup>12</sup> the angular parts of both the electron wave functions and transition matrix element are expanded in the spherical harmonics basis as

$$\psi_f(\mathbf{r}) = \sum_{l'm'} R_{l'm'}^f(r) Y_{l'm'}(\theta, \varphi) \quad (2)$$

and

$$e^{i\mathbf{q}\cdot\mathbf{r}} = 4\pi \sum_{l,m} i^l j_l(qr) Y_{lm}(\theta_q, \varphi_q) Y_{lm}^*(\theta, \varphi), \quad (3)$$

with  $R_{l'm'}^f(r) = \langle Y_{l'm'} | f \rangle$ . The initial core state is assumed to be *s* type, and the final state is usually a mixture of partial waves because of the ligand-field influence in a solid system. Substitution of these expansions into Eq. (1) separates the angular variables of the transferred momentum  $\mathbf{q}$  from its magnitude in  $S(\mathbf{q}, \omega)$  as

$$S(\mathbf{q}, \omega) = \sum_f \left| \sum_{lm} s_{flm}(q) Y_{lm}(\theta_q, \varphi_q) \right|^2 \delta(\Delta E - \hbar\omega), \quad (4)$$

where

$$s_{flm}(q) = i^l \sqrt{4\pi} \int_0^\infty j_l(qr) R_{lm}^f(r) R_0(r) r^2 dr \quad (5)$$

is the magnitude of the  $Y_{lm}$ -projected momentum space convolution between the initial state  $|0\rangle$  and each final state

$|f\rangle$ .<sup>6,27</sup> This approach is very similar to the formalism of Soinenen *et al.*,<sup>10</sup> but without using the muffin-tin approach employed in that work.

For the first three orders of spherical harmonics expansion ( $l$  up to 2), partial waves of  $Y_{00}$ ,  $Y_{1,\pm 1}$ ,  $Y_{20}$ , and  $Y_{2,\pm 2}$  could all have nonvanishing contributions to  $S(\mathbf{q}, \omega)$  for  $\mathbf{q} \perp c$ . Hence, the nonexistence of the exciton peak for  $S(\mathbf{q}, \omega)$  measured along  $\mathbf{q} \perp c$  for any magnitude of  $q$  indicates the absence of these partial waves. Also the  $Y_{2,\pm 1}$  do not have contributions to the XRS spectra along either direction. This leaves  $Y_{10}$  the only spherical harmonic component for  $l < 3$  to contribute to the  $\mathbf{q} \parallel c$  spectra.

This identification of a  $Y_{10}$ -type exciton is consistent with the fact that boron atoms sit only at sites with reflection symmetry about the  $a$ - $b$  basal plane, which demands that each final state be an eigenstate of the corresponding reflection parity.<sup>23</sup> For a predominantly  $Y_{10}$ -type exciton, other possible higher-order  $Y_{lm}$  components must possess the same reflection parity. This symmetry argument puts stringent restrictions on other possible spherical-harmonic components to the final state wave function. Note that  $Y_{00}$ ,  $Y_{1,\pm 1}$ ,  $Y_{20}$ , and  $Y_{2,\pm 2}$  all have even reflection parity about the  $a$ - $b$  plane, while only  $Y_{10}$  and  $Y_{2,\pm 1}$  have odd reflection parity. Given the additional reflection symmetry about the  $a$ - $c$  plane for boron sites (Fig. 1, inset),  $Y_{2,\pm 1}$  could also be excluded from the final state wave function, because of the different  $a$ - $c$  plane reflection parity in comparison with  $Y_{10}$ . Thus for  $l < 3$ , the exciton state has a purely  $Y_{10}$  type of wave function. This is our central result.

Compared to previous anisotropy studies by XANES and EELS that only excluded  $Y_{1,\pm 1}$  contributions because of the dipole selection rule,<sup>22</sup> the present  $\mathbf{q}$ -dependent XRS study provides a more complete picture of the exciton state characteristics as of dominantly  $p_z$ -type ( $Y_{10}$ ), with no  $s$ ,  $p_{x,y}$ , or  $d$  components. The above analysis, in which the  $\mathbf{q}$ -dependent XRS spectra may be qualitatively interpreted in the context of the constraints imposed by the crystal symmetry, should be generically applicable to the analysis of the angular characteristics of excitons in other high-symmetry single crystals.

#### IV. THEORETICAL CALCULATIONS

Seeking independent verification and further insight into the exciton's  $\mathbf{q}$  dependence, we performed two independent first principles theoretical calculations. First, we modified the FEFF8 code<sup>34</sup> to calculate the density of final states projected onto the individual spherical harmonics as  $\langle Y_{lm} | G(\mathbf{r}, \mathbf{r}', \omega) | Y_{lm} \rangle$ , with the core-hole effect included (Fig. 2). The calculation confirms our symmetry argument by showing no contribution from even reflection parity  $Y_{lm}$ 's and also indicates the  $l$ -DOS for other odd  $Y_{lm}$ 's with  $l$  up to 3 are negligibly small. This includes  $Y_{30}$ , which is the only other possible contributor to the  $\mathbf{q} \parallel c$  spectra for  $l$  up to 3. Note that the single  $Y_{10}$  characteristic of the wave function indicates the exciton state is localized at the scattering atom.

Second, we calculated the frequency and wave dependent dielectric response function  $\epsilon(\mathbf{q}, \omega)$  for  $h$ -BN near the boron  $K$  edge and over the measured momentum transfer range. The calculation used a computational Bethe-Salpeter equa-

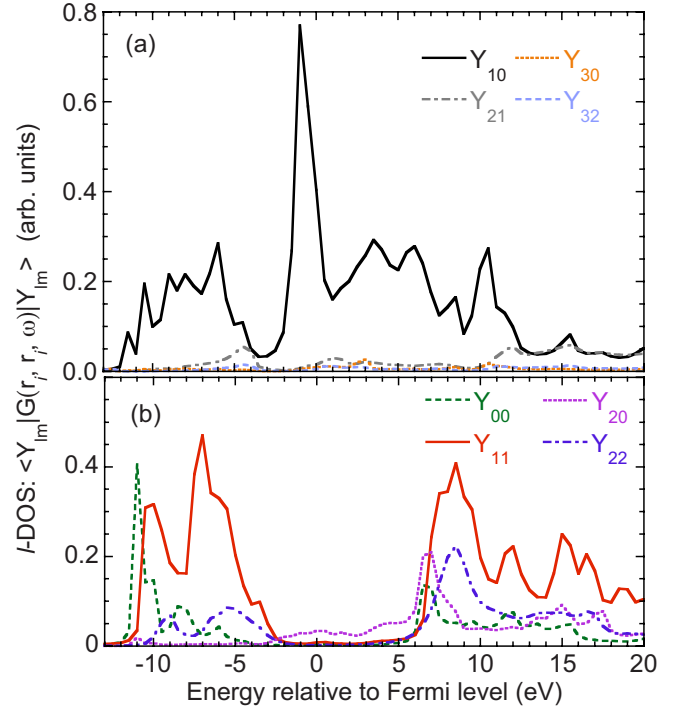


FIG. 2. (Color online) *Ab initio* FEFF8 calculation of the  $l$ -DOS onto different spherical harmonics with odd (top panel) and even (bottom panel) reflection parity about the basal plane for an  $h$ -BN cluster of 329 atoms.

tion (BSE) method for modeling core-excited states,<sup>32</sup> while including calculation of the GW self-energy<sup>1,9</sup> for both the energy-dependent quasiparticle shifts and the quasiparticle lifetime broadening. Convergence was checked with respect to the numerical cutoffs.<sup>35</sup> The calculated absolute values of  $\text{Im}[\epsilon(\mathbf{q}, \omega)]$  along both  $c$  and  $a$  axes are plotted in Fig. 3. For a core edge,  $\text{Re}[\epsilon(\mathbf{q}, \omega)]$  is very near to 1. The dynamical structure factor  $S(\mathbf{q}, \omega)$  is thus directly related to  $\text{Im}[\epsilon(\mathbf{q}, \omega)]$  as

$$S(\mathbf{q}, \omega) = -\frac{q^2}{4\pi e^2} \text{Im}[1/\epsilon(\mathbf{q}, \omega)] \approx \frac{q^2}{4\pi e^2} \text{Im}[\epsilon(\mathbf{q}, \omega)]. \quad (6)$$

We plot in Fig. 4 the integrated exciton intensity for energies below 194 eV from the BSE calculations and from the experimental data, normalized by the theoretical spectral weight as from the integration of  $\text{Im}[\epsilon(\mathbf{q}, \omega)]$  from 210 to 245 eV in Fig. 3. This combination of the experimental result and theoretical simulation represents our best estimation of the exciton  $q$ -dependence, considering the atomic background bears a  $q$  dependence<sup>10</sup> away from the  $q^2$  trend if summed only over a finite spectral range. The estimated relative standard uncertainty of the integrated intensity is 4% from a combination of statistical and estimated systematic background errors applying to each independent measurement. Since the theory has no lattice motion (phonon) included, the Frank-Condon effect from electron-phonon coupling<sup>4,36</sup> is not critical and the momentum is largely conserved during scattering.<sup>37</sup>

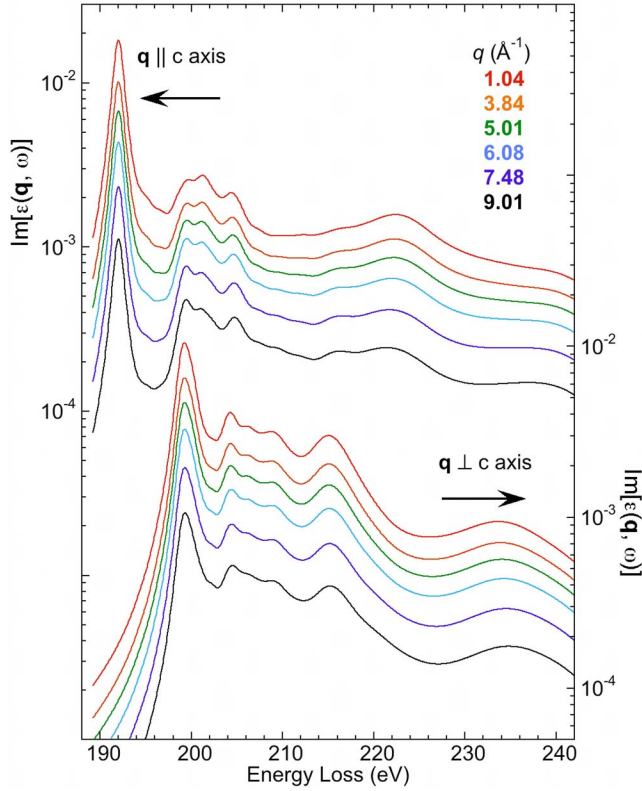


FIG. 3. (Color online) First-principles calculation of the absolute values of  $\text{Im}[\epsilon(\mathbf{q}, \omega)]$  over the experimentally measured  $q$  and  $\omega$  ranges along both  $\mathbf{q} \perp c$  and  $\mathbf{q} \parallel c$  directions.

Given the simple nature of the exciton state, it is interesting to calculate the  $q$  dependence of the dynamical structure factor  $S(q)/q^2$  from purely atomic models. For example, a crude model of transition between an  $1s$  and a hydrogenlike  $2p_z$  final state for a semiquantitative explanation can be considered as a first approximation. The  $S_{1s-2p_z}(q)$  is analytically expressed as<sup>6</sup>

$$S_{1s-2p_z}(q) \propto \left| \int_0^\infty j_1(qr) R_{2p}(r) R_{1s}(r) r^2 dr \right|^2 \propto q^2 / (k^2 + q^2)^6. \quad (7)$$

Here  $k = (Z + Z' / 2\epsilon) / a_0$ ,  $Z' = Z + 1$  is the equivalent atomic number for the core-hole potential, and  $\epsilon$  is the dielectric constant representing the effect of screening. For  $h$ -BN, the static dielectric constant  $\epsilon = 7$  represents a fully screened core hole, while  $\epsilon = 1$  represents a nonscreened core hole. We plot Eq. (7) with these two limits in Fig. 4, which should provide the boundary of the  $q$  dependence for the exciton state.

Significant improvements follow from more an advanced approach using sphericalized, self-consistent, density-functional calculations using the local-density approximation with the Vosko-Wilk-Nusair exchange-correlation functional<sup>38</sup> and an atomic program developed by Shirley.<sup>39</sup> Calculations were performed with the  $1s$  orbital computed in the initial state  $1s^2 2s^2 2p^1$ , and with the  $2p$  orbital computed in either the  $1s^1 2s^2 2p^1$  or  $1s^1 2s^2 2p^2$  final state. The former represents a fully delocalized state for the excited core electron,

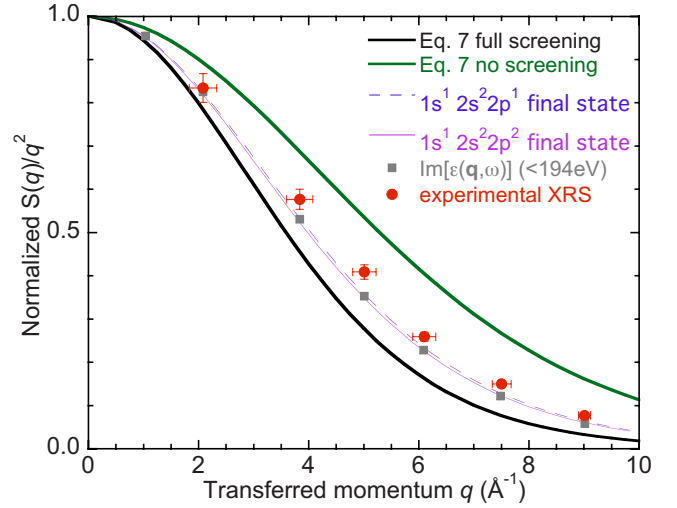


FIG. 4. (Color online) Normalized  $q$  dependence of the exciton intensity  $S(q)/q^2$ . Thick solid lines: Simple calculations of  $S(q)/q^2$  [Eq. (7)] using the boron  $1s$  core state and a hydrogenlike  $2p_z$  final state with a  $Z_{\text{boron}} + 1$  core hole, and  $\epsilon = 7$  and  $1$ , respectively (Ref. 6). Thin lines: Theoretically calculated  $S(q)/q^2$  for the exciton state, with either a delocalized final state  $1s^1 2s^2 2p^1$  (dashed thin line) or a bound final state  $1s^1 2s^2 2p^2$  (solid thin line). Solid squares: Integrated exciton intensity from BSE calculation (Fig. 3) from 190–194 eV. (Filled circles with error bars): Integrated exciton intensities from the experimental XRS data (Fig. 1, for energies below 194 eV), weighted by the calculated absolute values of  $\text{Im}[\epsilon(\mathbf{q}, \omega)]$  (Fig. 3) integrated over the 210–245 eV range. All curves are normalized to unity at  $q = 0$ .

while the latter case represents the excited electron being totally bound to its original site as in an isolated atom. These curves are plotted in Fig. 4, providing good agreement with the experimental results.

## V. CONCLUSION

In conclusion, we have used nonresonant x-ray Raman scattering (XRS) to perform exciton spectroscopy on  $h$ -BN, and find a  $Y_{10}$ -type exciton at the pre-edge position of the boron  $K$  shell spectra for  $\mathbf{q} \parallel c$ . This conclusion is supported by independent first principles calculations of the XRS and of the projected density of states. The existence of a pure-type exciton is strongly related to the presence of reflection symmetry in the system. This work illustrates the role of symmetry-based arguments in the interpretation of single-crystal  $\mathbf{q}$  dependent XRS studies and more broadly illuminates the interplay between local atomic symmetry and final-state effects in core-shell spectroscopies.

## ACKNOWLEDGMENTS

We acknowledge stimulating discussions with E. A. Stern, E. A. Miller, and B. D. Chapman. J.A.S. acknowledges financial support from the Academy of Finland under Contract No. 110571/1112642. This research was also supported by the L. X. Bosack and B. M. Kruger Charitable Foundation,

the Mellam Family Foundation, U.S. DOE Grants No. DE-FGE03-97ER45628 and No. DE-FG03-97ER45623 facilitated by the CMSN, and the Natural Sciences and Engineer-

ing Research Council of Canada. Use of the Advanced Photon Source is supported by the U.S. DOE-BES, under Contract No. DE-AC02-06CH11357.

\*yejun@aps.anl.gov

†seidler@phys.washington.edu

- <sup>1</sup>C.-O. Almbladh and L. Hedin, *Handbook on Synchrotron Radiation*, edited by E. E. Koch (North-Holland, Amsterdam, 1983), Vol. 1, Chap. 8.
- <sup>2</sup>M. S. Hybertsen and S. G. Louie, *Phys. Rev. Lett.* **55**, 1418 (1985); A. L. Ankudinov, A. I. Nesvizhskii, and J. J. Rehr, *Phys. Rev. B* **67**, 115120 (2003).
- <sup>3</sup>M. Rohlfiing and S. G. Louie, *Phys. Rev. B* **62**, 4927 (2000); S. Albrecht, L. Reining, R. Del Sole, and G. Onida, *Phys. Rev. Lett.* **80**, 4510 (1998).
- <sup>4</sup>A. Kivimäki, B. Kempgens, K. Maier, H. M. Köppe, M. N. Piancastelli, M. Neeb, and A. M. Bradshaw, *Phys. Rev. Lett.* **79**, 998 (1997).
- <sup>5</sup>K. Hämäläinen, S. Galambosi, J. A. Soininen, E. L. Shirley, J.-P. Rueff, and A. Shukla, *Phys. Rev. B* **65**, 155111 (2002).
- <sup>6</sup>Y. Feng, G. T. Seidler, J. O. Cross, A. T. Macrander, and J. J. Rehr, *Phys. Rev. B* **69**, 125402 (2004).
- <sup>7</sup>G. D. Mahan, *Phys. Rev.* **163**, 612 (1967); P. Nozières and C. T. De Dominicis, *ibid.* **178**, 1097 (1969).
- <sup>8</sup>H. P. Hjalmarson, H. Büttner, and J. D. Dow, *Phys. Rev. B* **24**, 6010 (1981); R. S. Knox, *Theory of Excitons* (Academic Press, New York, 1963).
- <sup>9</sup>J. A. Soininen, J. J. Rehr, and E. L. Shirley, *J. Phys.: Condens. Matter* **15**, 2573 (2003).
- <sup>10</sup>J. A. Soininen, A. L. Ankudinov, and J. J. Rehr, *Phys. Rev. B* **72**, 045136 (2005).
- <sup>11</sup>T. T. Fister, G. T. Seidler, L. Wharton, A. R. Battle, T. B. Ellis, J. O. Cross, A. T. Macrander, W. T. Elam, T. A. Tyson, and Q. Qian, *Rev. Sci. Instrum.* **77**, 063901 (2006).
- <sup>12</sup>Y. Mizuno and Y. Ohmura, *J. Phys. Soc. Jpn.* **22**, 445 (1967); S. Doniach, P. M. Platzman, and J. T. Yue, *Phys. Rev. B* **4**, 3345 (1971).
- <sup>13</sup>D. T. Bowron, M. H. Krisch, A. C. Barnes, J. L. Finney, A. Kaprolat, and M. Lorenzen, *Phys. Rev. B* **62**, R9223 (2000); Ph. Wernet, D. Nordlund, U. Bergmann, M. Cavalleri, M. Odelius, H. Ogasawara, L. Å. Näslund, T. K. Hirsch, L. Ojamäe, P. Glatzel, L. G. M. Pettersson, and A. Nilsson, *Science* **304**, 995 (2004).
- <sup>14</sup>M. H. Krisch, F. Sette, C. Masciovecchio, and R. Verbeni, *Phys. Rev. Lett.* **78**, 2843 (1997); A. Mattila, J. A. Soininen, S. Galambosi, and S. Huotari, G. Vankó, N. D. Zhigadlo, J. Karpinski, and K. Hämäläinen, *ibid.* **94**, 247003 (2005); M. Balasubramanian, C. S. Johnson, J. O. Cross, G. T. Seidler, T. T. Fister, E. A. Stern, C. Hamner, and S. O. Mariager, *Appl. Phys. Lett.* **91**, 031904 (2007).
- <sup>15</sup>C. Sternemann, J. A. Soininen, S. Huotari, G. Vankó, M. Volmer, R. A. Secco, J. S. Tse, and M. Tolan, *Phys. Rev. B* **72**, 035104 (2005); T. T. Fister, G. T. Seidler, C. Hamner, J. O. Cross, J. A. Soininen, and J. J. Rehr, *ibid.* **74**, 214117 (2006); H. Sternemann, J. A. Soininen, C. Sternemann, K. Hämäläinen, and M. Tolan, *ibid.* **75**, 075118 (2007).
- <sup>16</sup>C. Sternemann, M. Volmer, J. A. Soininen, H. Nagasawa, M. Paulus, H. Enkisch, G. Schmidt, M. Tolan, and W. Schülke, *Phys. Rev. B* **68**, 035111 (2003).
- <sup>17</sup>S. Galambosi, J. A. Soininen, K. Hämäläinen, E. L. Shirley, and C.-C. Kao, *Phys. Rev. B* **64**, 024102 (2001); P. Abbamonte, K. D. Finkelstein, M. D. Collins, and S. M. Gruner, *Phys. Rev. Lett.* **92**, 237401 (2004).
- <sup>18</sup>R. A. Gordon, G. T. Seidler, T. T. Fister, M. W. Haverkort, G. A. Sawatzky, A. Tanaka, and T. K. Sham, *Europhys. Lett.* **81**, 26004 (2008).
- <sup>19</sup>J. S. Lee, *J. Chem. Phys.* **67**, 3998 (1977); K. N. Klump and E. N. Lassette, *ibid.* **68**, 3511 (1978); A. C. de A. e Souza and G. G. B. de Souza, *Phys. Rev. A* **38**, 4488 (1988); A. P. Hitchcock, *Phys. Scr.* **T31**, 159 (1990); J. F. Ying, C. P. Mathers, K. T. Leung, H. P. Pritchard, C. Winstead, and V. McKoy, *Chem. Phys. Lett.* **212**, 289 (1993); I. G. Eustatiu, T. Tyliczszak, A. P. Hitchcock, C. C. Turci, A. B. Rocha, and C. E. Bielschowsky, *Phys. Rev. A* **61**, 042505 (2000).
- <sup>20</sup>J. A. Soininen, A. Mattila, J. J. Rehr, S. Galambosi, and K. Hämäläinen, *J. Phys.: Condens. Matter* **18**, 7327 (2006); T. T. Fister, Ph.D. dissertation, University of Washington, 2007; T. T. Fister, F. D. Vila, G. T. Seidler, L. Svec, J. C. Linehan, and J. O. Cross, *J. Am. Chem. Soc.* **130**, 925 (2008).
- <sup>21</sup>R. S. Pease, *Acta Crystallogr.* **5**, 356 (1952); R. S. Pease, *Nature (London)* **165**, 722 (1950).
- <sup>22</sup>R. D. Leapman, P. L. Fejes, and J. Silcox, *Phys. Rev. B* **28**, 2361 (1983); R. D. Leapman and J. Silcox, *Phys. Rev. Lett.* **42**, 1361 (1979).
- <sup>23</sup>B. M. Davies, F. Bassani, F. C. Brown, and C. G. Olson, *Phys. Rev. B* **24**, 3537 (1981); F. C. Brown, R. Z. Bachrach, and M. Skibowski, *ibid.* **13**, 2633 (1976).
- <sup>24</sup>A. Chaiken, L. J. Terminello, J. Wong, G. L. Doll, and C. A. Taylor, *Appl. Phys. Lett.* **63**, 2112 (1993).
- <sup>25</sup>N. Watanabe, H. Hayashi, Y. Udagawa, K. Takeshita, and H. Kawata, *Appl. Phys. Lett.* **69**, 1370 (1996).
- <sup>26</sup>A. W. Moore, *Nature (London)* **221**, 1133 (1969).
- <sup>27</sup>Y. Feng, Ph.D. thesis, University of Washington, 2003.
- <sup>28</sup>H. Sternemann, C. Sternemann, G. T. Seidler, T. T. Fister, A. Sakko, and M. Tolan, *J. Synchrotron Radiat.* **15**, 162 (2008).
- <sup>29</sup>D. Pines and P. Nozières, *The Theory of Quantum Liquids* (Benjamin, New York, 1966), Vol. 1.
- <sup>30</sup>J. Barth, C. Kunz, and T. M. Zimkina, *Solid State Commun.* **36**, 453 (1980); A. Mansour and S. E. Schnatterly, *Phys. Rev. B* **36**, 9234 (1987).
- <sup>31</sup>E. L. Shirley, *J. Electron Spectrosc. Relat. Phenom.* **110-111**, 305 (2000).
- <sup>32</sup>J. A. Soininen and E. L. Shirley, *Phys. Rev. B* **64**, 165112 (2001); J. A. Soininen, K. Hämäläinen, W. A. Caliebe, C.-C. Kao, and E. L. Shirley, *J. Phys.: Condens. Matter* **13**, 8039 (2001); J. A. Soininen, J. J. Rehr, and E. L. Shirley, *Phys. Scr.* **T115**, 243 (2005).
- <sup>33</sup>W. L. Schaich, *Phys. Rev. B* **8**, 4028 (1973).

- <sup>34</sup>J. J. Rehr and R. C. Albers, *Rev. Mod. Phys.* **72**, 621 (2000); A. L. Ankudinov, B. Ravel, J. J. Rehr, and S. D. Conradson, *Phys. Rev. B* **58**, 7565 (1998).
- <sup>35</sup>Spectra were calculated using 60 conduction band states with an 81 Ry plane-wave cutoff and 4096  $k$  points.
- <sup>36</sup>F. Occelli, M. Krisch, P. Loubeyre, F. Sette, R. Le Toullec, C. Masciovecchio, and J.-P. Rueff, *Phys. Rev. B* **63**, 224306 (2001); G. D. Mahan, *ibid.* **15**, 4587 (1977).
- <sup>37</sup>E. L. Shirley, *Phys. Rev. Lett.* **80**, 794 (1998).
- <sup>38</sup>S. H. Vosko, L. Wilk, and M. Nusair, *Can. J. Phys.* **58**, 1200 (1980); S. H. Vosko and L. Wilk, *Phys. Rev. B* **22**, 3812 (1980).
- <sup>39</sup>E. L. Shirley, Ph.D. dissertation, University of Illinois-Urbana Champagne, 1991.